

Excitability following an avalanche-collapse process

F. PLAZA¹, M. G. VELARDE¹, F. T. ARECCHI², S. BOCCALETTI², M. CIOFINI²
and R. MEUCCI²

¹*Instituto Pluridisciplinar, Universidad Complutense de Madrid
Paseo Juan XXIII, 1, 28040 Madrid, Spain*

²*Istituto Nazionale di Ottica, Largo E. Fermi, 6, 50125 Firenze, Italy*

(received 13 November 1996; accepted in final form 4 March 1997)

PACS. 02.30Hq – Ordinary differential equations.

PACS. 42.65Sf – Dynamics of nonlinear optical systems; optical instabilities, optical chaos, and optical spatio-temporal dynamics.

PACS. 42.60Gd – Q-switching.

Abstract. – Excitability and relaxation oscillations are shown to appear in the vicinity of subcritical or transcritical bifurcations with a different scenario from those previously introduced in biology, chemistry and liquid-crystal physics. Experimental observation of such a scenario has been done in a laser with intracavity saturable absorber.

Since the work by Hodgkin and Huxley on neurons [1], excitability has become a paradigm in biology as well as in non-linear chemistry and physics. A mathematical basis for excitability was provided by FitzHugh and Nagumo [2], [3]. The aim of this letter is to point out that excitability exists in a general class of systems where it has not been sought for and to show experimentally that a laser with a saturable absorber can behave as an excitable system. For such a system, a dynamical description has been provided [4]-[10], but so far no one had considered it in terms of excitability.

A dynamical system is excitable when a stationary solution is stable with regard to perturbations smaller than a characteristic threshold. If perturbed above this threshold, the system performs a large cycle, coming back to its resting initial state. In practical cases, it is necessary to apply an external perturbation to observe the dynamical cycle. Here we study such a dynamics close to a bifurcation from stationary to oscillatory behavior. There exist three generic bifurcations of this type in the plane [11], [12]: i) a Hopf bifurcation from an unstable focus, ii) a saddle-node bifurcation taking place on a closed path (saddle-node homoclinic bifurcation), and iii) a homoclinic bifurcation or saddle-loop bifurcation. Excitability is associated with each one of these bifurcations, which qualitatively correspond to three types of behavior, namely: i) FitzHugh-Nagumo dynamics (FHN) [2], [3] which exhibits a Hopf bifurcation with the so-called “canard” phenomenon [13]; ii) Coullet’s dynamics [14], [15], that uses a Ginzburg-Landau approach leading to an excitable regime in the vicinity of a saddle-node homoclinic bifurcation in oscillating systems close to a strong resonance; iii) the dynamics of

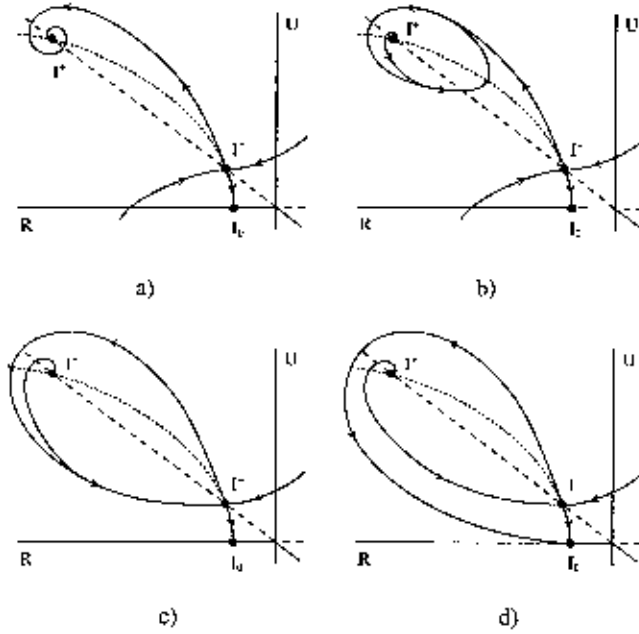


Fig. 1. – Schematic representation of typical phase space in an avalanche-collapse process, for $R_0 < 0$ and decreasing ε . *a)* Bistable regime; *b)* $\varepsilon < U_+$: past a Hopf bifurcation of I_+ ; *c)* at the ε value where the saddle loop homoclinic bifurcation occurs; *d)* excitable regime obtained beyond the homoclinic bifurcation. Dashed lines correspond to nullclines of eqs. (1).

systems with a homoclinic bifurcation having the excitable regime just after the disappearance of oscillations.

The three types of excitability appear after different bifurcations so they are topologically different [12]. Here we focus attention on type iii) (excitability following a homoclinic bifurcation), as it has not been studied previously. Suppose a system undergoes an inverse bifurcation: it can be either a transcritical or a subcritical pitchfork or a subcritical Hopf bifurcation. It is generally assumed that the energy supply which supports the bifurcation is powerful enough to maintain at a given value the control parameter of the bifurcation. In more realistic situations, the control parameter may vary according to the availability of the energy supply by a fixed flux.

The simplest case of such situation is the transcritical bifurcation. For this bifurcation, all the calculations are very simple to carry out and the dynamics is topologically the same as for subcritical pitchfork or Hopf bifurcations. We thus consider

$$\begin{cases} \partial_t U = RU + U^2, \\ \partial_t R = \varepsilon(R_0 - R - kU^2). \end{cases} \quad (1)$$

where U is the order parameter, R the control parameter, R_0 the value of R that would be fixed in the case of a very fast R dynamics independent of U , and ε the ratio of the characteristic time of U to the characteristic time of R . The first equation is the normal form of the bifurcation, the second equation describes the dynamics of R . When U vanishes, R is stable around R_0 ; as U increases, R decreases quadratically ($k > 0$). Below the threshold $R_0 = 0$, I_0 ($U = 0, R = R_0$) is a stable solution. Then for $1 + 4kR_0 > 0$, other stationary solutions exist created by an inverse saddle-node bifurcation: I_{\pm} defined by $U_{\pm} = -R_{\pm} = (1 \pm \sqrt{1 + 4kR_0})/2k$. These

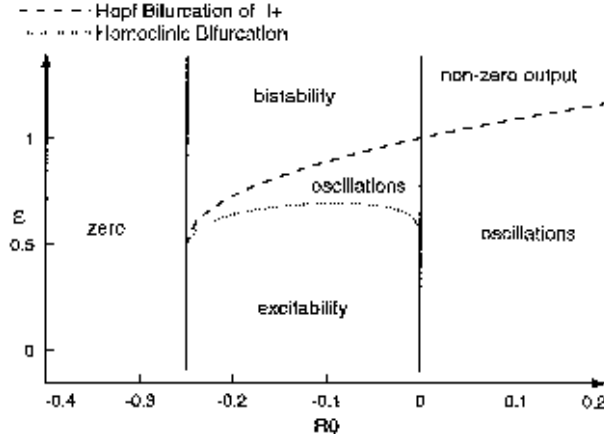


Fig. 2. – State diagram of eqs. (1) ($k = 1$).

solutions do not correspond to a bifurcation of the stationary solution I_0 . I_- is a hyperbolic point for all ε . I_+ is stable for $\varepsilon > U_+$ (fig. 1 a)). Note that this point is located on the unstable branch of the transcritical bifurcation diagram, but can be made stable. For $\varepsilon < U_+$, this point is destabilized via a Hopf bifurcation (fig. 1 b)). When ε is decreased, the limit cycle exists until it reaches the hyperbolic point I_- . Then the homoclinic bifurcation occurs, and the oscillations around I_+ disappear (fig. 1 c)). The only stable point remaining in the phase portrait is I_0 . Perturbations of I_0 beyond the stable manifold of I_- drive the system into a large excursion in phase space which goes beyond I_+ (fig. 1 d)) before coming back to I_0 . This dynamics corresponds exactly to the qualitative framework we fixed.

We restrain our study to $U > 0$, as the dynamics is invariant in the upper half plane, since the horizontal axis is invariant. Decreasing ε produces a destabilization of I_+ at the same value, but a homoclinic bifurcation is no longer possible. Oscillations appear with stronger and stronger relaxation features as $\varepsilon \rightarrow 0$. If $R_0 < 0$, the key parameter that produces the transition between oscillations and excitability is the characteristic time ε of the control parameter. Decreasing ε from unity changes the system dynamics through the following scenarios: non-zero stationary stable output, localized oscillations around a non-zero value and excitability. The state diagram of this system is summarized in fig. 2.

In the excitable ($R_0 < 0$) or oscillatory ($R_0 > 0$) regime, the structure of the pulse is the same. For ε small, the signal U grows exponentially, while R does not change in an appreciable manner. When U becomes of order unity, the control parameter suddenly decreases at a faster rate than U , since U acts quadratically on R . Then, R quickly stops the *avalanche* of U , and brings U back to zero. After this *collapse*, R slowly reaches its stable value R_0 .

This qualitative picture is not changed when one considers a subcritical Hopf or a subcritical pitchfork bifurcation. An interesting example of this latter case is the laser with intracavity saturable absorber (LSA). In a recent paper [16], it has been shown that starting from a minimal Maxwell-Bloch description [4]-[7], a state diagram similar to that reported in fig. 2 is obtained for LSA, topologically equivalent to model (1). For LSA, U represents the field amplitude and R the net gain (laser gain minus cavity losses minus saturable absorber losses). In R , the absorber losses saturate at increasing intensity U^2 . Thus, the equations become

$$\begin{cases} \partial_t U = RU - \beta U^3, \\ \partial_t R = \varepsilon(R_0 - R - kU^2). \end{cases} \quad (2)$$

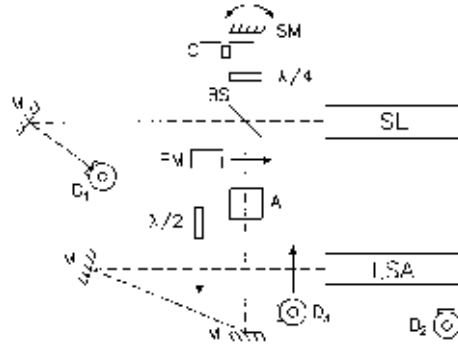


Fig. 3. – Experimental setup. LSA: CO₂ laser with an SF₆ saturable absorber; SL: stabilized CO₂ laser; M: mirrors; SM: scanning mirror; BS: 50 % beam splitter; PM: power meter; A: variable attenuator; D₁, D₂, D₃: fast HgCdTe detectors; $\lambda/2$: half-wave plate; $\lambda/4$: quarter-wave plate; C: rotating chopper wheel.

with $R_0 < 0$. Equations (2) imply a modification of fig. 2: the dashed line separating non-zero stationary output from oscillation bends down at large R_0 , as easily checked by writing the new Jacobian around I_+ and imposing the Hopf condition. As a result, the new state diagram can be obtained by decreasing R_0 at a fixed small ε , which yields sequentially: non-zero steady output, oscillations with non-zero average, excitability of the zero state. For type-ii) excitability, one would instead observe oscillations around zero followed by excitability [15].

For a sufficient pump power, the LSA offers various dynamical regimes like bistability and relaxation oscillations (passive Q-switching) [4]-[10]. If we now reduce the amount of pump, but inject an external signal, the LSA can be triggered to an avalanche-collapse excitability process, illustrated by an output independent of the input, down to a threshold injection below which no output appears.

Evidence of type-iii) excitability emerges from the experiment of fig. 3, where LSA denotes the CO₂ laser with an SF₆ saturable absorber, and SL a stabilized CO₂ laser. The time evolution of the LSA signal is monitored by means of the fast detector D₂; the mean output power emitted from the coupling mirror can be measured using a power meter (PM). The SL is a single-mode CO₂ laser, tuned on the same frequency of the LSA by inserting the half-wave plate ($\lambda/2$) and looking for beating on the detector D₁. During this operation, the variable attenuator A is removed. Decreasing the gain of the LSA via its pumping current i , the following behavior is observed: stationary non-zero output ($i \geq 10$ mA), weak oscillations around the non-zero output ($i = 9$ mA), growth of the oscillations \rightarrow passive Q-switching (type I-PQS [8], $i = 8$ mA) at a frequency around 1 kHz (fig. 4 a)), stationary zero output ($i \leq 4.5$ mA). Note that in the region $4.5 \text{ mA} \leq i \leq 8 \text{ mA}$, reducing the gain decreases the pulse repetition frequency while the pulse shape remains unchanged.

The excitability of the zero output state appears when we inject a weak signal from SL into LSA after reflection on a scanning mirror (SM). The injected light provides a perturbation to the zero state of LSA, that yields a big response if a threshold value is overcome. The SM (rotating at 4 kHz) and the chopper C provide an injection consisting of a sequence of pulses at a frequency of about 50 Hz. A quarter-wave plate ($\lambda/4$) provides the injected light with the appropriate horizontal polarization (the $\lambda/2$ plate has been removed). The configuration of fig. 3 prevents both lasers from auto-injection phenomena, hence the SM does not induce oscillations of LSA when the SL output is closed. The response of the LSA (solid line) to an injected signal (dashed line) is shown in fig. 4 b); the pulse shape is the same as that of fig. 4 a).

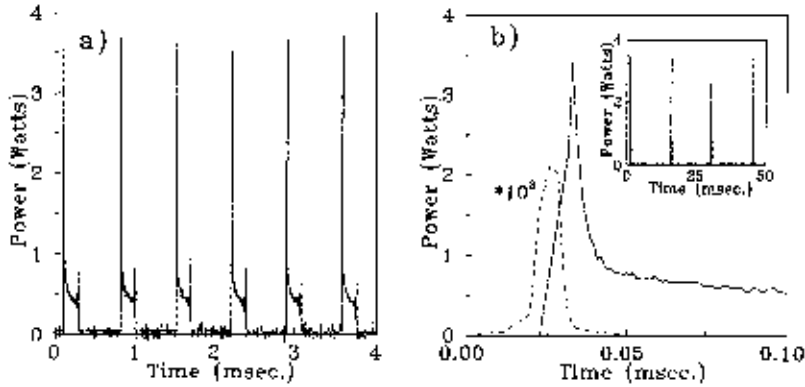


Fig. 4. – *a*) Passive Q-switching pulses of LSA for $i = 8$ mA, without injection. *b*) Single pulse response of LSA (solid line) for a small injected signal (dashed line) for $i = 4.5$ mA. The vertical scale for the injected signal is in mW. Inset: sequence of pulses due to injection. The after pulse plateaux at roughly 0.75 W lasts for a time of about 0.2 ms before the zero state is recovered. The repetition frequency (about 50 Hz, see text) is imposed by SM and C.

Three important features of the experiment identify excitability, linking the observations to the predictions of the theoretical model. First, the sequence of behaviors observed without injection for decreasing R_0 (that is the excitation current) is incompatible with type-ii) behavior. Second, at the excitation current $i = 4.5$ mA, an external injection recovers a giant output pulse, past a defined threshold. To estimate such a threshold, we remove C, measure with PM the average power before attenuator A and record the corresponding input to LSA with detector D_3 . Evaluating the ratio between the peak and average signals and taking into account the attenuation, we estimate a threshold of 0.25 ± 0.02 mW peak power. Third, mean height and shape of the pulses *do not* depend on the injected signal, provided the latter overcomes threshold. Clearly, these facts differ from the behavior of a light amplifier where the output has a shape depending on the input and displays no threshold.

We ought to emphasize that the quantitative results of the experiment, hence the specific form and related details of the pulse of fig. 4 *b*) are not fully described by the two variable model here introduced. Indeed, on the one hand the avalanche-collapse model does not account for the detuning and for the rotational manifold of CO_2 molecules. On the other hand the actual form of the pulses depends on the nature of the absorber as well as on the particular conditions of operation. The after-pulse (from 0.05 ms on in fig. 4 *b*)) is not a steady state but rather a long transient before the complete vanishing of the output (as can be appreciated from the inset) and is related to the slow decay of rotational levels [9], [17]-[20]. Yet, the reported experimental results are in qualitative agreement with the predictions of the above model.

In conclusion, the experiment here reported accommodates beautifully with the scenario of the avalanche-collapse model. In view of the generality of the mechanisms here considered, this new type of excitability may be of relevance in other realms of science. Recently, we learned of similar phenomena in a semiconductor laser with optical feedback [21].

This research was supported by European Union under grants ERBCHG-CT93-0404 and 107, by DGICYT (Spain) PB 93-81, by Fundación “Ramón Areces” and by Fundación BBV (Programa Cátedra Cambridge University).

REFERENCES

- [1] HODGKIN A. L. and HUXLEY A. F., *J. Physiol.*, **117** (1952) 500.
- [2] FITZHUGH R., *Biophys. J.*, **1** (1961) 445.
- [3] NAGUMO J., ARIMOTO S. and YOSHIZAWA S., *Proc. I. R. E.*, **50** (1962) 2061.
- [4] BURAK I., HOUSTON P. L., SUTTON D. G. and STEINFELD J. I., *IEEE J. Quantum Electron*, **QE-7** (1971) 73.
- [5] LUGIATO L. A., MANDEL P., DEMBINSKI S. T. and KOSSAKOWSKI A., *Phys. Rev. A*, **18** (1978) 238.
- [6] ANTORANZ J. C., GEA J. and VELARDE M. G., *Phys. Rev. Lett.*, **47** (1981) 1895.
- [7] ARIMONDO E., CASAGRANDE F., LUGIATO L. A. and GLORIEUX P., *Appl. Phys. B*, **30** (1983) 57.
- [8] ARIMONDO E., BOOTZ P., GLORIEUX P. and MENCHI E., *J. Opt. Soc. Am. B*, **2** (1985) 193.
- [9] TANJI K., TACHIKAWA M., KAJITA M. and SHIMIZU T., *J. Opt. Soc. Am. B*, **5** (1988) 24.
- [10] DE TOMASI F., HENNEQUIN D., ZAMBON B. and ARIMONDO E., *J. Opt. Soc. Am. B*, **6** (1989) 45.
- [11] ANDRONOV A. A., LEONTOVITCH E. A., GORDON I. I. and MAIER A. G., *Theory of Bifurcations of dynamic systems on a plane* (Wiley, New York, N.Y.) 1973.
- [12] KUZNETSOV Y. A., *Elements of Applied Bifurcation Theory* (Springer Verlag, New York, N.Y.) 1995, Chapt. 2.
- [13] DUMORTIER F., in *Bifurcations and periodic orbits of vector fields*, edited by D. SCHLOMIUK (Kluwer Academic Press, Dordrecht) 1993, pp. 19-73.
- [14] COULLET P., FRISCH T., GILLI J. M. and RICA S., *Chaos*, **4** (1994) 485.
- [15] COULLET P. and PLAZA F., *Int. J. Bif. Chaos*, **4** (1994) 1173.
- [16] PLAZA F. and VELARDE M. G., *Int. J. Bif. Chaos*, **6** (1996) 1873.
- [17] DUPRÉ J. and MEYER F. and MEYER C., *Rev. Phys. Appl. (Paris)*, **10** (1975) 285.
- [18] FOX A. G. and SCHWARTZ S. E. and SMITH P. W., *Appl. Phys. Lett.*, **12** (1968) 371.
- [19] HENNEQUIN D., DE TOMASI F., ZAMBON B. and ARIMONDO E., *Phys. Rev. A*, **37** (1988) 2243.
- [20] NEVDAKH V. V., GAIKO O. L. and ORLOV L. N., *Opt. Comm.*, **127** (1996) 303.
- [21] GIUDICI M., GREEN C., GIACOMELLI G., NESPOLO U. and TREDICCE J. R., preprint.